The 6th Annual IEEE International Conference on
Cyber Technology in Automation, Control and Intelligent Systems
June 19-22, 2016, Chengdu, China

Design of Vision-based Obstacle Crossing of High-voltage Line Inspection Robot*

Yanhuan Zhu, Xin Wang* and Bo Xu
School of Mechanical Engineering and Automation
Harbin Institute of Technology Shenzhen Graduate School
Shenzhen, China
**Corresponding Author: wangxinsz@hit.edu.cn*

***Abstract*—High-voltage inspection robot can detect and identify various obstacles while it is walking along the high-voltage line and plan specific bypassing strategy for different types of obstacles. In this paper vision-based obstacle recognition algorithms are studied based on visual sensors specifically for the unique features of 500kv high-voltage wire. Considering the texture features owned by high-voltage wire in a complex background, the algorithms combining grey co-occurrence matrix (GLCM) and fuzzy C- means clustering algorithms (FCM) are used to extract the texture features and segment the high-voltage wire. Then the image HSV features are used to achieve recognition of the driving wheels for independent hanging-on-line operation by the inspection robot. Also SVM classification is combined with additional structural constraints and type of obstacle can be accurately identified. The experimental results show that the algorithms can reliably identify the torsional damper, spacers and suspension clamp. The robot can be guided to bypass obstacles.**

Keywords—inspection robot; obstacle recognition; structural constraint

I. INTRODUCTION

Under the condition of the high-voltage charged line, inspection robot is researched for walking on wire with the wheels with the sensors to implement close inspection for wire, as in [1]. But because there are obstacles installed in lines such as torsional damper, spacer, suspension clamp, they would stop the operations of the robot, which will greatly limit the workspace and efficiency of the robot. In order to complete the inspection task, the robot should recognize the types of obstacles with sensors and cross obstacles.

At present, there are two methods to recognize the obstacle for inspection robot. One is multiple sensors data fusion navigation technology. Peters etc. [2] installed 34 accessible sensors on the inspection robot to detect the obstacle. The researchers in Tokyo electric power company used maps navigation and combined with the feedback of ultrasonic sensor and accessible sensor to control obstacle crossing of inspection robot in [3, 4]. IREQ carried out the development of high-voltage line deicing robot whose action of obstacle crossing mainly depended on the camera installed on the robot via remote operation, as in [5~8]. Zhongwei Chen put forward a navigation method with electromagnetic sensor for inspection robot discussed in [9, 10], but this method was restricted by detection range of electromagnetic sensor. Another one is vision-based obstacle crossing technology. Peungsungwal etc. [11] used the camera installed on the inspection robot to achieve the recognition of insulator. Based on the geometric characteristics of the obstacles, Xiaoming Xiong designed vision-based algorithms of obstacle recognition, as in [12]. In view of structural features of transmission line, Yunchu Zhang put forward visual navigation algorithms of obstacle recognition based on structural constraint, as in [13].

According to inspection robot's navigation task, in this paper the vision-based algorithms is put forward for obstacle crossing. The rest of the paper is structured as follows. Section Ⅱ presents the system of the inspection robot. Section Ⅲ describes the algorithms of vision-based obstacle crossing. Section Ⅳ describes the experiment of the algorithms of obstacle crossing. And section Ⅴ presents the conclusion and the direction of future work.

II. INSPECTION ROBOT SYSTEM

A. Description of Robot Structure

A high-voltage inspection robot is mainly composed of three arms and a robot control box, which is shown in Fig. 1(a). Supporting arm shown in Fig. 1(b) contains driving wheel and clamping wheel, which guarantees that robot could climb the slope with a certain gradient and avoid falling from the wire. And the assistant arm is used to guarantee that there are at least two arms hanging on the cable while the robot is crossing obstacle.

There are 4 CCD cameras installed on the inspection robot. Three of them installed on the bottom of robot arms are used to guide motion of driving wheels. The remaining camera installed on the forward of the control box is used to recognize the type of obstacles and detect fault of high-voltage lines. Master control board placed in the control box processes the image acquired from the camera and outputs the result signals which are used to guide the robot to complete inspection task.

B. Obstacle Crossing of the Inspection Robot

The inspection robot shown in the Fig. 1 is able to walk steadily on high-voltage line with the help of driving wheels and clamping wheels. When confronted with obstacles such as torsional damper, spacer or insulator, the inspection robot is required to cross them. The obstacle-crossing process designed in this paper is described as follows.

978-1-5090-2733-0/16/$31.00 © 2016 IEEE

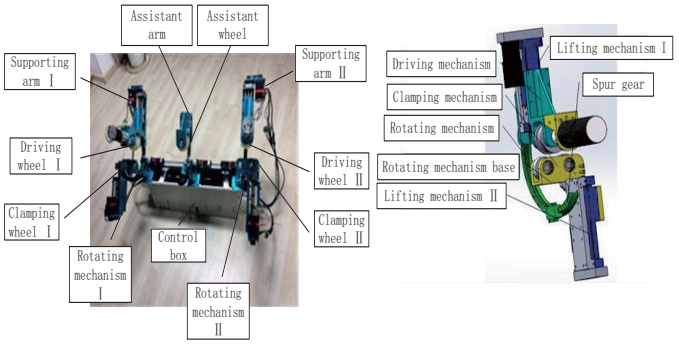

(a) Structure of robot (b) Supporting arm

Fig. 1. Structure of high-voltage inspection robot.

In step Ⅰ when the line inspection robot is operating on the line, the ultrasonic distance sensor detects the presence of obstacle in front of it. For step Ⅱ the visual obstacle recognition system is activated, determining the type of obstacle and corresponding bypassing plan. For Step Ⅲ the clamping wheel on supporting arm Ⅱ clamps the high-voltage line. The clamping and the driving wheels on supporting arm Ⅰ respectively move upward and downward to detach from the line. In step Ⅳ the spur gears on supporting arm Ⅰ rotate to a certain angle to cross the obstacle, and the supporting arm Ⅱ drives the robot to move forward while the supporting arm Ⅰ bypassing the obstacle. In step Ⅴ under the help of visual surveillance, spur gears on supporting arm Ⅰ rotate to a certain angle to push the driving wheel above the high-voltage line and the driving and clamping wheels clamp the wire. In step Ⅵ the driving and clamping wheels are used to support arms to move downward and keep the clamping status, then the forcing the roller on assistant arm can roll off the high-voltage line. The spur gear on assistant arm rotates to a certain angle, driving wheels of supporting arms move forward thus enabling the middle arm successfully bypassing the obstacle. In step Ⅶ the spur gears on supporting arm rotate to a certain angle, rendering the roller above the high-voltage line. Driving and clamping wheels of both supporting arms move upward while keeping clamped, so that the assistant arm could hang over the wire. In step Ⅷ repeating the process from step Ⅲ to step Ⅴ, then supporting arm Ⅱ could bypass the obstacle, thus the whole robot successfully overcome the obstacle.

C. Control System of the Inspection Robot

The high-voltage inspection robot requires relatively higher stability. The control system shown in Fig. 2 mainly consists of three parts. They are human-computer interaction part, wireless communication part and robot control part.

III. Algorithms of Vision-based Obstacle Crossing

According to the obstacle-crossing process of high-voltage line robot, the algorithms of vision-based obstacle crossing should complete two tasks as follows. One task is to recognize the position of the center line of high-voltage line and driving wheel, and guide the precise action of driving wheels' hanging on line. Another one is to recognize types of obstacles, such as torsional damper, spacer and suspension clamp.

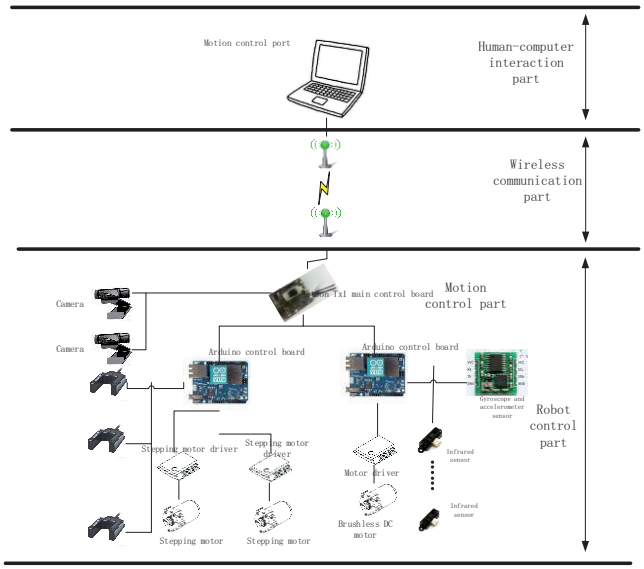

Fig. 2. Diagram of control system.

The primary goal of the hanging on line algorithms of the driving wheels is to make the distance from central point of driving wheel to high-voltage wire central line less than the given range. So the driving wheel and high-voltage wire are chosen as recognition targets as is shown in Fig. 3.

A. Recognition of Driving Wheel

As shown in Fig. 3, the driving wheel has a distinctive color feature which is also highly contrastive comparing to the environment. And the image area of driving wheel is constant during the process. Also, the camera position is deliberately set to make the position of the driving wheel in the image remain unchanged. The flow chart of driving wheel recognition algorithm is shown in Fig. 4 and the recognition results are shown in Fig. 5.

Implementing the algorithm proposed in this paper, the result shown in Fig. 5(e) comes out that driving wheel is successfully retrieved. The geometric center of the contour curve of the driving wheel contour curve is given in (1) and (2).

$$x_c = (\sum(x,y) \in c^x)/(\sum(x,y) \in c) \quad (1)$$

$$y_c = (\sum(x,y) \in c^y)/(\sum(x,y) \in c) \quad (2)$$

where c is the set of driving wheel contour curve pixel, x_c is the horizontal coordinate of geometric center of driving wheel and $y_c$is the vertical coordinate of geometric center of the driving wheel.

B. Recognition of High-voltage Line

By analyzing the wire in Fig. 3, the results of the following features are obtained. One of features is that the high-voltage line lies throughout the entire image. Another feature is that high-voltage line has a specific width in the image. The third feature is that high-voltage line itself has a very systematic texture information. The working environment of dealing with 500kv high-voltage wire is highly complicated, so the fuzzy C-means clustering (FCM) algorithm is adopted in this paper.

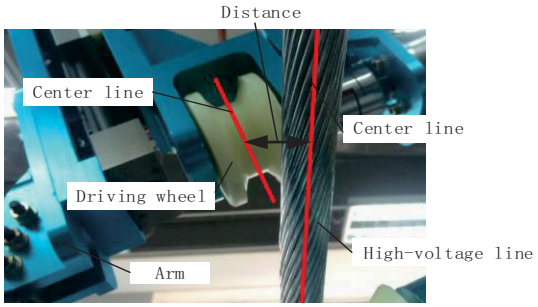

Fig. 3. Relative position of driving wheel and high-voltage line.

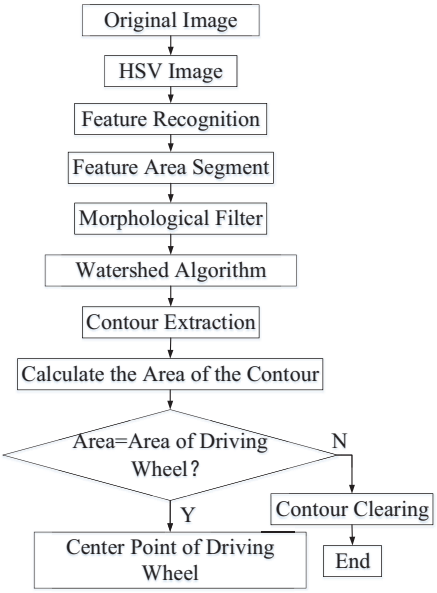

Fig. 4. Flow chart of recognition algorithm of driving wheel.

The FCM algorithm can solve the problem of setting threshold. Another advantage of FCM is that it is free of artificial intervention. Traditional FCM uses the picture's tri-channel pixel value or grey value as eigenvector inputs to conduct clustering and segmentation, as in [14]. However, the shooting situation can be largely influenced by the environmental light, rendering the texture and brightness uneven, thus it's unavailable here to simply use pixel value only as eigenvector inputs.

This paper chooses the eigenvalue of the grey co-occurrence matrix (GLCM) as inputs of FCM. GLCM is the matrix function of the pixel distance and angle by calculating the correlation of a certain distance and direction of two pixel point. It reflects the image's integrated information in the direction and speed, as in [15, 16]. GLCM is a method to enhance the texture feature. After calculating GLCM, we often calculate the eigenvalue of the GLCM to represent texture feature. Considering the characteristics of eigenvalue of the GLCM, in this paper inverse differential matrix, angular second moment and entropy are chosen to represent the text feature of high-voltage line.

The inverse differential matrix (IDM) reflects the clarity and rule of the texture. It is defined as follows.

$$IDM = \sum p(i,j)/(1+(i-j)^2) \tag{3}$$

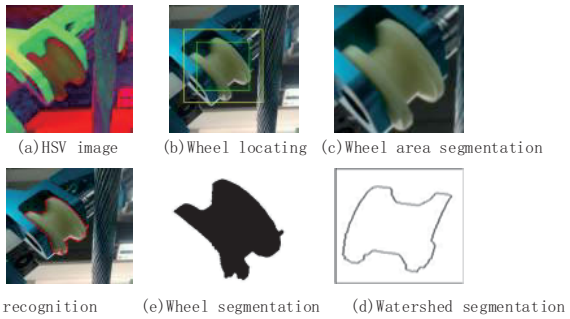

Fig. 5. Recognition result of driving wheel.

The entropy (ENT) is a measure of the amount of information that is used to describe the image, which indicates the complexity of the image. It is denoted as follows.

$$ENT = \sum(p(i,j) \times (-logp(i,j))) \tag{4}$$

The angular second moment (ASM) is a measure of the degree of uniformity and texture of the image and given by.

$$ASM = \sum p^2(i,j) \tag{5}$$

The entropy, inverse differential matrix, and angular second moment of GLCM are used as the regional texture features measure to segment wire from the image. The flow chart of segmentation of wire is shown as Fig .6.

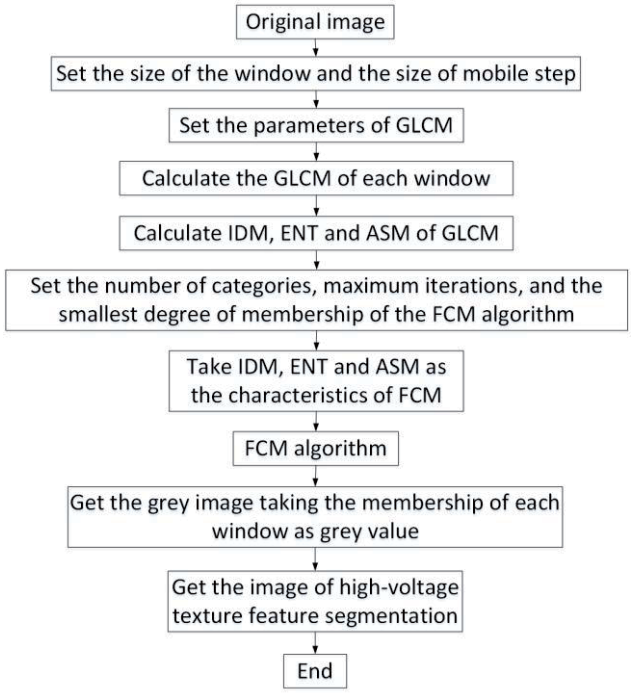

Fig. 6. Flow chart of recognition algorithm of high-voltage wire.

C. *Wire Centre Line Fitting Using Least Square Method*

As described above, the texture area of the high-voltage wire is composed of discrete points. The method in this paper is aimed at retrieving the center line of the wire. Here the least square method is adopted.

The traditional least square method is to minimize the weighted average value of the square of distances. The distance is the difference between each point and the well-fitting curve of the line. In this paper, due to high-voltage wire's specific position and features, the traditional least square is unavailable in some situation.

The upper left corner of the image is defined as the origin of coordinates, the horizontal direction as the x-axis, and the vertical direction as the y-axis. The wire center line equation is giving by,

$$x = a_0 + a_1 y \tag{6}$$

where a_0 and a_1 are the parameters of the line equation.

The moderation from the traditional least square is to minimize the weighted sum of square of horizontal distance between each point and the well-fitting curve of the line. That is

$$min \sum_{i=1}^{N} [x_i - (a_0 + a_1 y_i)]^2 \tag{7}$$

Where a_0 and a_1 are rearranged and stated as follows,

$$\frac{\partial}{\partial a_0} \sum_{i=1}^{N} [x_i - (a_0 + a_1 y_i)]^2 = 0 \tag{8}$$

$$\frac{\partial}{\partial a_1} \sum_{i=1}^{N} [x_i - (a_0 + a_1 y_i)]^2 = 0 \tag{9}$$

Substituting and reorganizing, we have

$$-2 \sum_{i=1}^{N} [x_i - (a_0 + a_1 y_i)] = 0 \tag{10}$$

$$2 \sum_{i=1}^{N} y_i [x_i - (a_0 + a_1 y_i)] = 0 \tag{11}$$

$$\begin{cases} \sum_{i=1}^{N} x_i - N a_0 - a_1 \sum_{i=1}^{N} y_i = 0 \\ \sum_{i=1}^{N} x_i y_i - a_0 \sum_{i=1}^{N} y_i - a_1 \sum_{i=1}^{N} y_i^2 = 0 \end{cases} \tag{12}$$

Solving the equations the solutions are given as follows,

$$\dot{a_0} = \frac{(\sum_{i=1}^{N} y_i \sum_{i=1}^{N} x_i y_i - \sum_{i=1}^{N} x_i \sum_{i=1}^{N} y_i^2)/()}{(\sum_{i=1}^{N} y_i)^2 - N \sum_{i=1}^{N} y_i^2} \tag{13}$$

$$\dot{a_1} = \frac{\sum_{i=1}^{N} x_i \sum_{i=1}^{N} y_i - N \sum_{i=1}^{N} x_i y_i}{(\sum_{i=1}^{N} y_i)^2 - N \sum_{i=1}^{N} y_i^2} \tag{14}$$

Thus the result of the center line of the high-voltage wire is obtained.

After retrieving the pose position and orientation of driving wheel and high-voltage wire, we get the distance error between them

$$e = |x_c + \dot{a_1} y_c + \dot{a_0}| / |\dot{a_1}| \tag{15}$$

D. Description of Obstacles On the Wire

Fig. 7 shows the structure of four-cracking type 500kv wire. The typical obstacles that an inspection robot would encounter are spacer, suspension clamp and torsional damper. However, those types of obstacles have neither rich surface texture features nor distinct color characteristics. Also, they are hinged with the high-voltage wires, which altogether makes it hard to be divided into separate areas. But there's still some geometric features shown in the image like circles and straight lines. Those features have certain positional relationship with each other and the high-voltage wire. Thus in this paper, the method of combining SVM as in [17] and the structural constraints of obstacles is adopted for recognition algorithm.

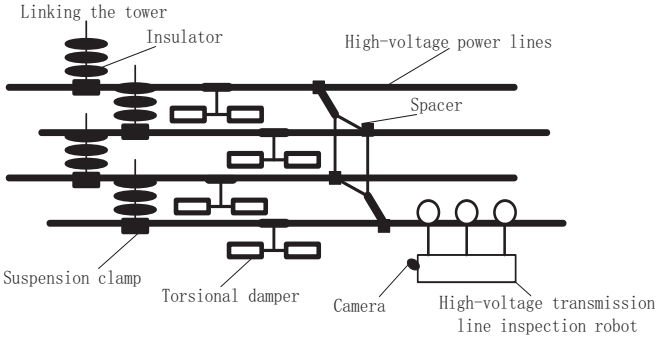

Fig. 7. Schematic diagram of typical obstacles on high-voltage line.

The algorithm of obstacle recognition includes two main steps. That is rough recognition and precise recognition. In the rough recognition, SVM is used to get the classifier and the classifier is used to get the obstacle region. Then in the precise recognition the positional relationship between the obstacles with the high-voltage wire and the obstacles' innate structure features is built as structural constraints for the recognition of the obstacles.

E. Rough Recognition of the Obstacle

In this paper the positive and negative samples ratio of 1: 3 are chosen to train samples to get a relatively accurate classifier.

The sample selection criteria are different backgrounds and different lighting conditions but all the same size. In the process, sample images are shot from different angles and manually cut into uniform size of 20 × 20 pixel. The total sample size of this paper is 1000 for positive sample and 3000 for negative sample. And the torsional damper sample is shown in Fig. 8. Then a classifier is acquired. And the next step is to detect the position of the obstacle in the images obtained by camera, the detection results are shown in Fig. 9.

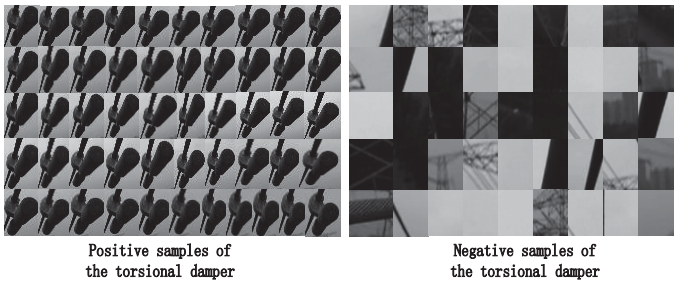

Fig. 8. Torsional damper sample.

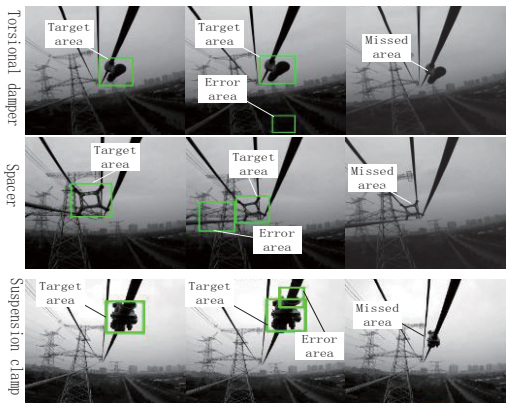

Fig. 9. Detection results of obstacles.

F. *Precise Recognition of the Obstacle*

As shown in Figure 8, there exists false detection or missed cases in the detection process, thus in this paper structural constraints are chosen to further confirm the types of obstacles.

The torsional damper is installed below the high-voltage wire, which is assembled together by two hollow cylinders and appears in the image as round arc shapes. Using its certain radius and certain positional relationship with high-voltage wire, the torsional damper can be detected in which circle the arc belongs to as is shown in Fig.9.

As shown in Fig. 10, circle features are detected and the radius and the circle center position are retrieved. Then the detected circle is tested whether it fits the structural constraints. Thus the torsional damper can be found. The structural constraints are given as follows.

$$\begin{cases} w < r < 3 \times w \\ 0 < d < 4 \times w \end{cases} \tag{16}$$

where w is the width of wire, r is the radius of the circle and d is the distance of circle center to high-voltage wire centre.

As shown in Fig. 11, the spacer is used to connect four-cracking high-voltage wires. Spacer images captured by the camera have certain characteristics of a plane. For image area segmented by classifier, the algorithm of this paper is to extract the closed contours of the image. Depending on the spacer's particular contour of its middle part or the area size of the circumscribed square, the interfering contours could be get rid of. Then the center point of the remaining contour and its distance to the wire are searched, thus the recognition of spacer is obtained. The constraints are shown as follows,

$$\begin{cases} 60 \le l \le 80 \\ 45 \le s \le 65 \\ 6 \times w \le a \le 8 \times w \end{cases} \tag{17}$$

where l is the length of the circumscribed quadrilaterals, s is the width of the circumscribed quadrilaterals and a is the centre of the circumscribed quadrilaterals to high-voltage wire.

Suspension clamp is installed below the wire, which is the metal fitting connecting the wire and the insulators. Suspension clamp itself is relatively small with no obvious identifiable surficial structural features. The algorithm in this paper is to segment the classifier identified area firstly. Then the edge contour of the suspension clamp is extracted. Next the interference factor is removed based on the contour area size. And then the contours of the center line are fitted from the remaining discrete points based on its distance to the center line of high-voltage, suspension clamps can be recognized. The result is shown in Fig. 12. And the constraints are shown as follows,

$$\begin{cases} 3500 \le A \le 5000 \\ 0 \le b \le w \end{cases} \tag{18}$$

where A is the area size of the contour image of the suspension clamp and b is the distance from the center of contour to center line of the high-voltage line.

IV. Experiment

The recognition algorithms are tested as shown in Fig. 13. The experiments results show that the algorithms can accurately help to extract the center line of high-voltage wire and guide the inspection robot based on the distance from driving wheel center to the high-voltage wire center line.

In the obstacle recognition experiments, the images of the obstacle are from different angles and have various changing position, shape and size.

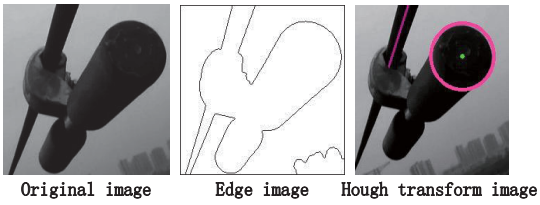

Fig. 10. Precise Recognition of torsional damper.

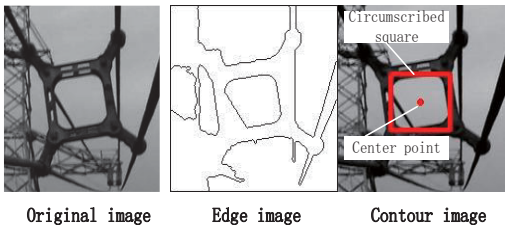

Fig. 11. Precise Recognition of the spacer.

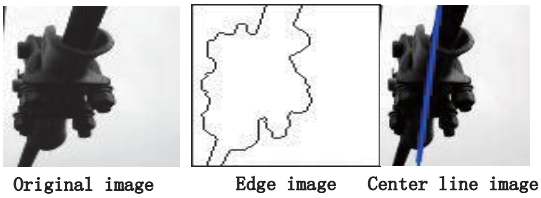

Fig. 12. Precise Recognition of suspension clamp.

In order to test the recognition effects of the obstacles, the experiments are carried out with different distances and different angles under all kinds of types of obstacles. The results are shown in Fig. 8 to Fig. 12. In the paper 150 images are chosen

to conduct the experiment. As indicated in table Ⅰ, the proposed method of combing the SVM classifier with the structural constraints can significantly identify the types of obstacles.

However, in hundreds of experiments, there did exist a couple of times where this algorithm failed to recognize the obstacles. When the robot faced with unrecognizable obstacle images, a human-computer interaction program would be activated. The wireless image transmission device carried by the robot would transmit the image information and assistance requests to the ground control agent, the failed-to-identify image would be identified manually and recognition result would be feedback to the robot.

V. Conclusion

In this paper the algorithms are studied based on the extracted vision features information of driving wheels, high-voltage wires and obstacles for the inspection robot. By using the method of combining SVM classification with additional structural constraints, the types of obstacles can be accurately and effectively identified.

Experiments show that the algorithms under normal light and simple background are effective. However in the environment with too strong light, the problem of false detection exists. Therefore, further improvements are studied of its adaptability of multi-scale images. The implementation of visual, optical fiber sensors is required with the information on surroundings. The method of combining with multi-sensor data fusion will enhance the robustness of the inspection robot.

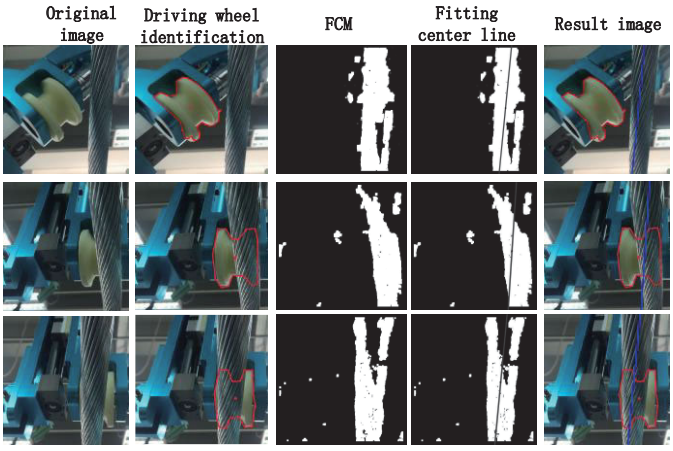

Fig. 13. Experimental results in the laboratory.

TABLE I. Results of Recognition of Obstacles

Method	Accuracy rate (%)		
	torsional damper	spacer	suspension clamp
SVM+structure constraints	96	93.33	92.67

References

[1] J. Katrasnik, F. Pernus, and B. Likar, "A survey of mobile robots for distribution power line inspection", IEEE Transactions on Power Delivery, vol. 25, No. 1, pp.485-493, 2010.

[2] Peters J F, Ahn T C, Borkowskii M. Obstacle Classification by a Line-Crawling Robot: a Rough Neurocomputing Approach[C]// Proceedings of the Third International Conference on Rough Sets and Current Trends in Computing-Lecture Notes in Artificial Intelligence. London, UK: Springer-Verlag, 2002, pp. 594-601.

[3] Jun Sawada, Kazuyuki Kusumoto, Tadashi Munakata. A mobile robot for inspection of power transmission lines[J]. IEEE Transactions on Power Delivery. 1991.6(1): 309-315.

[4] Kobayashi H, Nakamura H, Shimada T. An inspection robot for feeder cables-basic structure and control[C]// Industrial Electronics, Control and Instrumentation, 1991. Proceedings. IECON '91, 1991 International Conference on IEEE, 1991:992-995, vol.2.

[5] Montambault S, Cote J, St. Louis M. Preliminary results on the development of a teleoperated compact trolley for live-line working[C]// Transmission and Distribution Construction, Operation and Live-Line Maintenance Proceedings. 2000 IEEE ESMO-2000 IEEE 9th International Conference on IEEE, 2000: 21-27.

[6] Montambault S, Pouliot N. The HQ LineROVer: contributing to innovation in transmission line maintenance[C]// Transmission and Distribution Construction, Operation and Live-Line Maintenance, 2003. 2003 IEEE ESMO. 2003 IEEE 10th International Conference on IEEE, 2003:33-40.

[7] Pouliot N, Montambault S. Geometric design of the LineScout, a teleoperated robot for power line inspection and maintenance[C]// Robotics and Automation, 2008. ICRA 2008. IEEE International Conference on IEEE, 2008:3970-3977.

[8] Toth J, Pouliot N, Montambault S. Field experiences using LineScout Technology on large BC transmission crossings[C]//Applied Robotics for the Power Industry (CARPI), 2010 1st International Conference on IEEE, 2010:1-6.

[9] CHEN, Zhong-wei, XIAO Hua, and WU Gong-ping. "Electromagnetic sensor navigation system of robot for high-voltage transmission line inspection[J].Transducer and Microsystem Technologies 9 (2006): 30-39.

[10] Wu, G. P, et al. "Development of a mobile inspection robot for high voltage power transmission line." Automation of Electric Power Systems 30.13 (2006): 90-93.

[11] Peungsungwal S, Pungsiri B, Chamnongthai K, et al. Autonomous robot for a power transmission line inspection[C]//ISCAS 2001, The 2001 IEEE International Symposium on Circuits and Systems, Sydney, NSW Australia, 2001: 121-124.

[12] Xiong, Xiao-Ming, et al. "Automation recognition of obstacles on power transmission line." Chinese High Technology Letters, 15.2(2005):39-42.

[13] Li, Quan-Min, Yun-Chu Zhang, and Jun-Ce Li. "Visual navigation for power transmission line inspection robot." Jisuanji Gongcheng yu Yingyong (Computer Engineering and Applications) 42.19 (2007): 221-224.

[14] CHUANG K S, TZENG H L, CHEN S, et a1.Fuzzy c-means clustering with spatial information for image segmentation. Computerized Medical Imaging and Graphics(S0895−6111), 2006, 30(1):9-15.

[15] Robert M Haralick, Karthikeyan Shanmugam, Its' Hak Dinstein. Textural features for image classification. Systems, Man and Cybernetics, IEEE Transactions on, 1973(6):610-621.

[16] Robert M Haralick. Statistical and structural approaches to texture. Proceedings of the IEEE, 1979, 67(5): 786-804.

[17] John C. Fast Training of SVM Using Sequential Minimal Optimization Advances in Kernel Methods Support Vector Machine. Cambridge Boston, MA, USA: MIT Press, 1999.